Published in final edited form as:
J Magn Reson Imaging. 2010 May ; 31(5): 1230–1235. doi:10.1002/jmri.22140.

Whole-heart coronary MRA at 3.0 T using short-TR SSFP VIPR

Jingsi Xie, BS[1], **Peng Lai, Ph.D.**[1], **Himanshu Bhat, MS**[1], and **Debiao Li, Ph.D.**[1]
[1] Departments of Radiology and Biomedical Engineering, Northwestern University, Chicago, IL

Abstract

Purpose—To evaluate the feasibility of improving 3.0T steady-state free precession (SSFP) whole-heart coronary magnetic resonance angiography (MRA) using short-TR VIPR (Vastly Undersampled Isotropic Projection Reconstruction).

Materials and Methods—SSFP is highly sensitive to field inhomogeneity. VIPR imaging uses non-selective RF pulse, allowing short TR and reduced banding artifacts, while achieving isotropic 3D resolution. Coronary artery imaging was performed in 9 healthy volunteers using SSFP VIPR. TR was reduced to 3.0 ms with an isotropic spatial resolution of $1.3 \times 1.3 \times 1.3$ mm^3. Image quality, vessel sharpness and lengths of major coronary arteries were measured. Comparison between SSFP using Cartesian trajectory and SSFP using VIPR trajectory was performed in all volunteers.

Results—Short-TR SSFP VIPR resulted in whole-heart images without any banding artifacts, leading to excellent coronary artery visualization. Average image quality score for VIPR-SSFP was 3.12 ± 0.42 out of 4 while that for Cartesian SSFP was 0.92 ± 0.61. A significant improvement ($p < 0.05$) in image quality was shown by Wilcoxin comparison. The visualized coronary artery lengths for VIPR-SSFP were: 10.13 ± 0.79 cm for the left anterior descending artery (LAD), 7.90 ± 0.91 cm for the left circumflex artery (LCX), 7.50 ± 1.65 cm for the right coronary artery (RCA), and 1.84 ± 0.23 cm for the left main artery (LM). The lengths statistics for Cartesian SSFP were 1.57 ± 2.02 cm, 1.54 ± 1.93 cm, 0.94 ± 1.17 cm, 0.46 ± 0.53 cm respectively. The image sharpness was also increased from 0.61 ± 0.13 (mm^{-1}) in Cartesian-SSFP to 0.81 ± 0.11 (mm^{-1}) in VIPR-SSFP.

Conclusion—With VIPR trajectory, TR is substantially decreased, reducing the sensitivity of SSFP to field inhomogeneity and resulting in whole-heart images without banding artifacts at 3.0T. Image quality improved significantly over Cartesian sampling.

Keywords

MR studies; coronary vessel; 3.0T; steady-state free precession; radial sampling

Introduction

SSFP has been the method of choice for coronary MRA at 1.5T because of its intrinsically high SNR and CNR (1). Studies have demonstrated that SSFP sequences provide excellent vessel visualization, increased vessel sharpness and increased vessel length compared with gradient echo sequences (1–3). SSFP coronary MRA has also been attempted at 3.0T (4), however, due to the increased B_o and B_1 field inhomogeneities (5) the results were variable. Many techniques have been developed to address these problems. To compensate for B_1 inhomogeneities and achieve uniform T_2 preparation of the magnetization across the imaged

Please send proof and correspondence to: Debiao Li, Ph.D., 737 N. Michigan Ave., Suite 1600, Chicago, IL 60611, Tel: (312) 926-4245, Fax: (312) 896-5665, d-li2@northwestern.edu.

volume, adiabatic RF pulses were used in the T_2 preparation scheme (6). Phase-encoding steps were paired to reduce flow-related phase perturbations (7). A flip angle sweep according to a Kaiser-Bessel weighted function (8) in conjunction with a fifth-order binomial pulse (9) proved to be an effective magnetization preparation scheme because it could provide homogenous excitation across a range of off-resonance frequencies. Schär etl al. also used localized shimming and resonance frequency determination based on a measured B_0-map (10) to acquire breath-hold SSFP cine images at 3.0 T.

However, the major challenge for SSFP at 3.0 T is its sensitivity to increased field inhomogeneity (11–13). This sensitivity is dependent on the repetition time (TR). The signal passband for SSFP is inversely proportional to TR. In particular, signal nulls occur every 1/TR in resonance frequency, producing “banding” artifacts in the images. Nayak et. al. suggested a method to widen the passband of SSFP beyond 1/TR by alternating the repetition time (14).

Another way is to reduce TR, which will widen the usable bandwidth of SSFP and cover a broader range of off-resonance frequencies. The method we proposed to achieve this goal is to use Vastly Undersampled Isotropic Projection Reconstruction (VIPR) trajectory (16,17), which employs a non-selective RF pulse to reduce TR. So combining VIPR trajectory with SSFP will result in short TR, which may improve image quality at 3.0 T by increasing the passband and reduce the banding artifacts. VIPR has previously been used for coronary MRA at 1.5T (16). The advantages of VIPR for coronary MRA are: i) isotropic spatial resolution, which allows subsequent reformatting of any slice of interest and results in better coronary artery visualization (18), ii) capability of undersampling with benign aliasing artifacts, which allows the imaging time to be reduced significantly, iii) reduced sensitivity to motion artifacts compared with Cartesian sampling (16).

The purpose of the work was to evaluate the feasibility of whole-heart coronary MRA at 3.0T using SSFP and to verify that short TR with VIPR allows improved coronary MRA. Volunteers studied were performed to determine whether this technique can visualize the coronary arteries with better quality than conventional Cartesian SSFP technique.

Materials and Methods

All studies were conducted on a 3.0T Magnetom Trio scanner (Siemens Healthcare, Erlangen, Germany). The scanner has a bore diameter of 60 cm and is capable of operating at a maximum gradient strength of 40 mT/m and slew rate of 200 mT/m/ms. Nine healthy volunteers without known history of cardiac disease (five males, 22–47 years old, mean age 31 years) were recruited for this study. Written consent was obtained before each study, in compliance with our Institutional Review Board guidelines.

Sequence Design

The sequence is based on the ECG-triggered, navigator-gated SSFP (19), as illustrated in Fig.1a. Due to the increased B_1 inhomogeneity at 3.0 T, an adiabatic T_2 preparation (6) was used to achieve uniform blood-myocardium contrast. It consists of a hard 90° RF pulse, followed by a pair of adiabatic full-passage refocusing pulses and then another 90° hard tip up pulse. The duration of the entire T_2-preparation was 40 ms. It was followed by a navigator acquisition on the dome of the right hemidiaphram. A ± 3 mm acceptance window and prospective real-time adaptive motion correction was applied with a correction factor of 0.6 in the superior–inferior direction (20). To achieve uniform fat suppression in the presence of increased B_1 inhomogeneity at 3.0T an adiabatic full passage Spectral Presaturation Inversion Recovery (SPIR) (21,22) pulse was employed with an optimized shift frequency of −750 Hz and flip angle of 110°. Fifteen sinusoidal preparation pulses

were applied prior to imaging data acquisition to reduce transient signal oscillations (23). Nonselective RF pulses were used for spin excitation (Fig. 1b). Isotropic coverage of 3D k-space was obtained by distributing the end points of the projections along a spiral running on the sphere from pole to equator (Fig.1c) (17). An isotropic spatial resolution of 1.3 mm^3 was used, resulting in a TR of 3 ms. To minimize the off-resonance artifacts, a frequency scouting method was used to determine the optimal synthesizer frequency (24).

Three-Dimensional Coronary Artery Imaging

3D whole-heart coronary MRA using VIPR was acquired on each volunteer. For comparison purposes, whole-heart Cartesian coronary MRA were acquired as well. The order in which Cartesian and VIPR scans were acquired was randomized to eliminate potential timing bias.

All imaging acquisitions were performed under free breathing with the subjects in a supine position. Two dimensional (2D) scout images were first obtained in three orthogonal orientations using low-resolution, single-shot FLASH sequence (TR = 3.2 ms, TE = 1.5 ms, resolution = 4.2 × 2.1 × 5.0 mm^3, in-plane field of view (FOV) = 400×400 mm^2, slice thickness = 5 mm, flip angle (FA) = 8°). These scout images were used to identify the position of the heart and diaphragm. A cine scan was then prescribed in the four-chamber view to determine the quiescent period for coronary artery imaging (25). Parameters for the cine scout included TR/TE = 4.0/2.0 ms, FOV = 360 × 360 mm^2, resolution = 1.9 × 1.9 × 6.0 mm^3, and FA = 15°. Images were acquired with a generalized autocalibrating partially parallel acquisition (GRAPPA) (26) acceleration factor of 2. Forty cardiac phases were reconstructed for visual assessment of global cardiac motion to determine the trigger delay time and the duration of acquisition window per heartbeat. Subject-specific field shimming and frequency adjustment (10) were also performed.

VIPR—VIPR scans were acquired using a three-dimensional SSFP sequence with radial sampling. Typical parameter values were as follows: TR/TE/flip angle = 3.0 ms/1.5 ms/50~60 degrees, bandwidth = 868 Hz/pixel, FOV = 356 mm^3, matrix size = 288 × 288 × 288, spatial resolution = 1.3 × 1.3 × 1.3 mm^3, number of projections = 11520 projections (undersampling factor of 8 compared with Nyquist sampling), readout points per projections = 288. Navigator was applied prospectively and the acceptance window was 3. All scans were synchronized to the cardiac cycle using electrocardiography (ECG) gating and navigator-gated. The total imaging time ranged from 7 to 12 minutes based on heart rate and breathing pattern.

3D Cartesian Sampling—3D Cartesian sampling scans were then performed using a three-dimensional single-slab SSFP sequence with the identical imaging parameter as previous 3D radial sampling except it followed the 3D Cartesian trajectory. The 3D k-space data were collected with a centric ordering scheme in the phase-encoding direction, and linear order in the partition-encoding direction. Eighty transverse slices were acquired. The spatial resolution was 1.3 × 1.3 × 1.3 mm^3. To speed up the image acquisition and keep imaging time comparable to VIPR, parallel data acquisition (GRAPPA) was used in the phase-encoding direction with an acceleration factor of 2. Other imaging parameters were: TR/TE/flip angle = 3.6 ms/1.8 ms/50~60°, readout bandwidth = 868 Hz/pixel. The total imaging time ranged from 7 to 13 minutes based on heart rate and breathing pattern.

To assess the field distribution of the heart, a 2D dual-echo gradient-echo sequence was used to calculate the phase image. Parameters for this sequence were: TR = 290.0 ms, TE_1 = 2.4 ms, TE_2 = 4.8 ms, (when water and fat are in-phase), segments = 48, readout bandwidth = 628 Hz/pixel, resolution = 1.8 × 1.8 × 3.0 mm^3, FOV = 229 × 330 mm^2, slice thickness = 3 mm, FA = 15°.

Data Analysis

Image Reformatting—VIPR image reconstructions were performed off-line using Matlab (Version 7.0, The Mathworks, Inc., Natick, MA). For image comparison, Multi-planar reconstructions (MPRs) were performed using the standard software in the Siemens imaging system. Whole-heart coronary MRA images were reformatted with the CoronaViz software (Siemens Corporate Research, Princeton, NJ, USA) to project multiple vessels onto a single image (27).

Statistical Analysis—To compare the image quality between VIPR and Cartesian trajectories, two MRI physicians with extensive coronary experiences blindly scored the images per patient based on a 4-point scale (28). The scoring scale and criteria for evaluation were as follows: 1 = poor delineation or uninterpretable coronary vessels (coronary artery with markedly blurred borders or edges), 2 = good (coronary artery vessels visible, but moderately blurred), 3 = very good (coronary artery clearly visible but blurring is still mildly present), and 4 = excellent (coronary artery visible, well delineated and sharply defined with no visible artifacts). The final quantitative results of these images are determined as the mean of grading. In addition, the lengths of visualized coronary arteries and image sharpness were measured using previously described methods (29,30). At last among 9 paired-slices between VIPR and Cartesian, Wilcoxin test was used to evaluate the differences in image grades between images acquired with VIPR sampling pattern and with Cartesian sampling. P-value < 0.05 was considered statistically significant. SNR and CNR analysis were not measured in this work because parallel data acquisition was used in Cartesian sampling, which made calculation of SNR and CNR unreliable.

Results

Major coronary arteries from nine volunteers were successfully visualized. To show the image quality that can be acquired using SSFP with VIPR trajectory at 3.0T and better visualize coronaries, reformatted images from two volunteers are show in Fig 2. The LAD, LCX and RCA are clearly depicted. Good contrast between blood and myocardium plus strong blood signal intensity are achieved. There are no banding artifacts present.

Fig. 3 shows two axial slices from the same volunteer using the VIPR trajectory (b and d) and Cartesian trajectory (a and c). The significantly decreased off-resonance artifacts with the VIPR trajectory are evident. For the Cartesian case (a and c), the image quality varies significantly and although the blood signal and contrast are reasonable due to use of SSFP sequence, off-resonance artifacts impede the visualization of the coronary arteries. In contrast, the VIPR trajectory (b and d) presents substantially better image quality, homogeneous blood pool signal and sharp delineation of the coronary arteries.

The off-resonance frequency map in the heart in one sample slice is shown in Fig. 4. The frequency in this slice ranges from −167 to 149 Hz. This exceeds the SSFP passband of ±138 Hz (for a 3.6 ms TR with Cartesian sampling), but is still in the SSFP passband of ±166.5 Hz (for a 3.0 ms TR with VIPR sampling).

The average image quality score for VIPR sampling was 3.12 ± 0.42 suggesting very good image quality, and that for Cartesian sampling was 0.92 ± 0.61suggesting poor image quality. In 9 volunteers, Wilcoxin test of the difference between VIPR and Cartesian sampling showed a highly significant increase ($p < 0.05$) in image quality. The visualized coronary artery lengths and image sharpness using both VIPR SSFP and Cartesian SSFP are summarized in Table 1. The depicted length and sharpness of coronary arteries were also significantly improved with VIPR trajectory,

Discussion

Contrast-enhanced whole-heart coronary MRA with gradient echo readout (31,32) has been proven to be a very promising technique at 3T. However, emerging evidence that links gadolinium-based contrast agents to nephrogenic systemic fibrosis (NSF) (33) has spurred a resurgence in non-contrast coronary MRA techniques, even though their quality is not yet comparable to contrast-enhanced imaging. SSFP is the method of choice for non-contrast MRA because of its intrinsically high SNR and CNR. But due to its high sensitivity to field inhomogeneities, SSFP has not yet been successfully applied for whole-heart imaging at 3T. This work described an initial attempt to improve whole-heart non-contrast SSFP imaging at 3.0T by employing VIPR trajectory with SSFP acquisition.

Isotropic spatial resolution whole-heart coronary MRA with short-TR SSFP VIPR at 3.0 T is proven to be feasible. Compared to conventional Cartesian SSFP, VIPR requires similar or even shorter imaging time. Image quality, image sharpness and depicted vessel length are significantly improved by VIPR trajectory. With TR decreased to 3.0 ms banding artifacts are substantially reduced as compared to Cartesian imaging at 3.0 T.

Several methods have been proposed to alleviate SSFP sequence-related imaging artifacts, such as optimizing synthesizer frequency to reduce off-resonance-related image artifacts (25), minimizing field inhomogeneity by employing localized shimming (10), or improving uniformity of T2 preparation using adiabatic T2 preparation pulse (6). These methods have improved SSFP sequence at 3.0T to a certain degree. However, there are limitations to these modifications and the image quality of 3.0T coronary MRA with Cartesian SSFP remains variable.

Volunteer studies in this work show that with short-TR SSFP VIPR, consistent coronary MRA image quality can be obtained at 3.0T. The main reason for improved image quality with VIPR is that due to the non-selective excitation TR is reduced. For banding-free imaging, the range of tolerable off-resonance frequencies has to be confined to ±1/(2TR). With TR decreasing from 3.6 ms for Cartesian to 3.0 ms for VIPR, the passband increases from 277 Hz to 333 Hz. Schar et al (34) suggested that whole-heart peak-to-peak field inhomogeneity differences at 3.0 T could be as large as 287.3Hz. Increased passband with VIPR allows coverage of the entire off-resonance frequency range, effectively eliminating the banding artifacts and substantially improving the image quality. To further reduce TR, asymmetric sampling along the readout direction can be considered. Another advantage of VIPR trajectory is its motion insensitivity. A comparative study on 1.5T shows that radial SSFP reduces motion artifacts and improves vessel delineation as compared to Cartesian SSFP (35).

Like other whole-heart techniques, one of the main problems with VIPR coronary MRA is the long acquisition time, particularly at relatively high image resolution. Parallel imaging should be employed to reduce imaging time and reduce potential artifacts related to cardiac and respiratory motion. With improved imaging speed, further improvement in spatial resolution to sub-mm will be possible.

In conclusion, whole-heart coronary MRA at 3.0 Tesla using short-TR SSFP VIPR is feasible and it results in whole-heart images without any banding artifacts, leading to excellent coronary artery visualization.

Acknowledgments

Supported in part by National Institute of Health grants nos. NIBIB EB002623 and NHLBI HL38698, and Siemens Medical Solutions USA, Inc., Malvern, PA.

References

1. Deshpande VS, Shea SM, Laub G, Simonetti OP, Finn JP, Li D. 3D magnetization-prepared true-FISP: a new technique for imaging coronary arteries. Magn Reson Med. 2001; 46:494–502. [PubMed: 11550241]
2. Shea SM, Deshpande VS, Chung YC, Li D. Three-dimensional True- FISP imaging of the coronary arteries: improved contrast with T2- preparation. J Magn Reson Imaging. 2002; 15:597–602. [PubMed: 11997902]
3. Weber OM, Martin AJ, Higgins CB. Cartesian, spiral, and radial coronary MR angiography - a comparison. J Cardiovasc Magn Reson. 2003; 5:188–189.
4. Bi X, Deshpande V, Simonetti O, Laub G, Li D. Three-dimensional breathhold SSFP coronary MRA: a comparison between 1.5T and 3.0T. J Magn Reson Imaging. 2005; 22:206–212. [PubMed: 16028242]
5. Dougherty L, Connick TJ, Mizsei G. Cardiac imaging at 4 Tesla. Magn Reson Med. 2001; 45:176–178. [PubMed: 11146502]
6. Nezafat, Reza; Stuber, Matthias; Ouwerkerk, Ronald, et al. B1-insensitive T2 preparation for improved coronary magnetic resonance angiography at 3 T. Magn Reson Med. 2006; 55:858–864. [PubMed: 16538606]
7. Bieri O, SchefflerBieri K. Flow Compensation in Balanced SSFP Sequences. Magn Reson Med. 2005; 54:901–907. [PubMed: 16142709]
8. Le Roux P. Simplified model and stabilization of SSFP sequences. Journ Magn Reson. 2003; 163:23–37.
9. Foxall DL. Starter Sequence for Steady-State Free Precession Imaging. Magn Reson Med. 2005; 53:919–929. [PubMed: 15799066]
10. Schar M, Kozerke S, Fischer SE, Boesiger P. Cardiac SSFP imaging at 3 Tesla. Magn Reson Med. 2004; 51:799–806. [PubMed: 15065254]
11. Carr HY. Steady-state free precession in nuclear magnetic resonance. Phys Rev. 1958; 112:14.Oppelt A, Graumann R, Barfuss H, Fischer H, Hartl W, Shajor W. FISP–A new fast MRI sequence. Electromedica. 1986; 54:15–18.
12. Freeman R, Hill HDW. Phase and intensity anomalies in Fourier transform NMR. J Magan Reson. 1971; 4:366–383.
13. Zur Y, Stokar S, Bendal P. An analysis of fast imaging seqnences with steady-state transverse magnetization refocusing. Magn ResonMed. 1988; 6:175–193.
14. Nayak, Krishna S.; Lee, Hsu-Lei; Hargreaves, Brian A.; Hu, Bob S. Wideband SSFP: Alternating Repetition Time Balanced Steady State Free Precession with Increased Band Spacing. Magn Reson Med. 2007; 58:931–938. [PubMed: 17969129]
15. Conolly, Steven; Nishimura, Dwight; Macovski, Albert. Variable-rate Selective Excitation. Journ Magn Reson. 1988; 78:440–458.
16. Barger AV, Block WF, Toropov Y, Grist TM, Mistretta CA. Time-resolved contrast-enhanced imaging with isotropic resolution and broad coverage using an undersampled 3D projection trajectory. Magn Reson Med. 2002; 48:297–305. [PubMed: 12210938]
17. Wong ST, Roos MS. A strategy for sampling on a sphere applied to 3D selective RF pulse design. Magn Reson Med. 1994; 32:778–784. [PubMed: 7869901]
18. Botnar RM, Stuber M, Kissinger KV, Manning WJ. Free-breathing 3D coronary MRA: the impact of “isotropic” image resolution. J Magn Reson Imaging. 2000; 11(4):389–93. [PubMed: 10767067]
19. Deshpande VS, Chung YC, Zhang Q, Shea SM, Li D. Reduction of transient signal oscillations in true-FISP using a linear flip angle series magnetization preparation. Magn Reson Med. 2003; 49(1):151–157. [PubMed: 12509831]
20. Wang Y, Ehman RL. Retrospective adaptive motion correction for navigator-gated 3D coronary MR angiography. J Magn Reson Imaging. 2000; 11(2):208–214. [PubMed: 10713956]
21. Zee CS, Segall HD, Terk MR, et al. SPIR MRI in spinal diseases. J Comput Assist Tomogr. 1992; 16:356–360. [PubMed: 1592915]

22. Halligan S, Healy JC, Bartram CI. Magnetic resonance imaging of fistula-in-ano: STIR or SPIR. Br J Radiol. 1998; 71:141–145. [PubMed: 9579177]

23. Paul, D.; Hennig, J. Comparison of different flip angle variation functions for improved signal behavior in SSFP sequences. Proc 12th Annual Meeting ISMRM; Kyoto, Japan. 2004. p. 2663

24. Deshpande, Vibhas S.; Shea, Steven M.; Li, Debiao. Artifact Reduction in True-FISP Imaging of the Coronary Arteries by Adjusting Imaging Frequency. Magn Reson Med. 2003; 49:803–809. [PubMed: 12704761]

25. Weber OM, Martin AJ, Higgins CB. Whole-heart steady-state free precession coronary artery magnetic resonance angiography. Magn Reson Med. 2003; 50:1223–1228. [PubMed: 14648570]

26. Griswold MA, Jakob PM, Heidemann RM, et al. Generalized autocalibrating partially parallel acquisitions (GRAPPA). Magn Reson Med. 2002; 47:1202–1210. [PubMed: 12111967]

27. Aharon, S.; Oksuz, O.; Lorenz, C. Simultaneous projection of multibranched vessels with their surroundings on a single image from coronary MRA. Proceedings of the 14th Annual Meeting of ISMRM; Seattle, WA, USA. 2006. (Abstract 365)

28. Kim WY, Danias PG, Stuber M, et al. Coronary magnetic resonance angiography for the detection of coronary stenoses. N Engl J Med. 2001; 345:1863–1869. [PubMed: 11756576]

29. Li D, Carr JC, Shea SM, Finn JP, et al. Coronary arteries: magnetization-prepared contrast-enhanced three dimensional volume-targeted breath-hold MR angiography. Radiology. 2001; 219:270–277. [PubMed: 11274569]

30. Bi X, Li D. Coronary Arteries at 3.0 T: Contrast-Enhanced Magnetization-Prepared Three-Dimensional Breathhold MR Angiography. J Magn Reson Imaging. 2005; 21:133–139. [PubMed: 15666400]

31. Bi X, Carr JC, Li D. Whole-heart coronary magnetic resonance angiography at 3 Tesla in 5 minutes with slow infusion of Gd-BOPTA, a high-relaxivity clinical contrast agent. Magn Reson Med. 2007; 58 :1–7. [PubMed: 17659628]

32. Yang Q, Li K, Liu X, Bi X, Liu Z, An J, Zhang A, Jerecic R, Li D. Contrast-enhanced whole-heart coronary magnetic resonance angiography at 3.0-T: a comparative study with X-ray angiography in a single center. J Am Coll Cardiol. 2009; 54:69–76. [PubMed: 19555843]

33. Prince MR, Zhang HL, Roditi GH, Leiner T, Kucharczyk W. Risk factors for NSF: a literature review. J Magn Reson Imaging. 2009; 30:1298–308. [PubMed: 19937930]

34. Schär, M.; Kozerke, S.; Boesiger, P. Considerations on Shimming for Cardiac Applications at 1.5 and 3.0T. Proceedings of the 11th Annual Meeting of ISMRM; Toronto, ON, Canada. 2003. (Abstract 174)

35. Spuentrup, Elmar; Katoh, Marcus; Buecker, Arno, et al. Free-breathing 3D Steady-State Free Precession Coronary MR Angiography with Radial k-Space Sampling: Comparison with Cartesian k-Space Sampling and Cartesian Gradient-Echo Coronary MR Angiography—Pilot Study. Radio. 2004; 231:581–586.

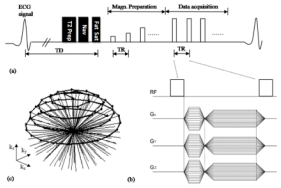

Figure 1.

(a) Schematic of the pulse sequence used for SSFP VIPR whole-heart coronary MRA. Adiabatic T_2-prep, Navigator (Nav), and Spectral Presaturation Inversion Recovery (SPIR) fat saturation pulses were applied prior to imaging. Fifteen sinusoidal preparation pulses were applied prior to imaging to reduce transient signal oscillations. (b) G_X, G_Y and G_Z between RF hard pulse represent gradients along the three orthogonal axes forming the VIPR trajectory. (c) k-space coverage with the VIPR trajectory. Black dots represents signal acquired.

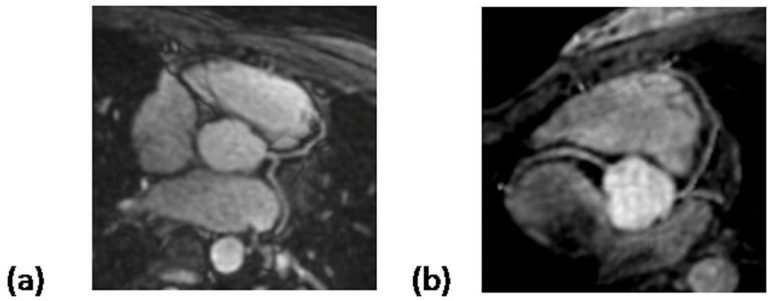

Figure 2.
Reformatted coronary artery images in healthy volunteers. (a) 47-year-old, 185-pound male volunteer. (b) 24-year-old, 125-pound female volunteer. Note that images show good image quality, and no apparent off-resonance or motion artifacts.

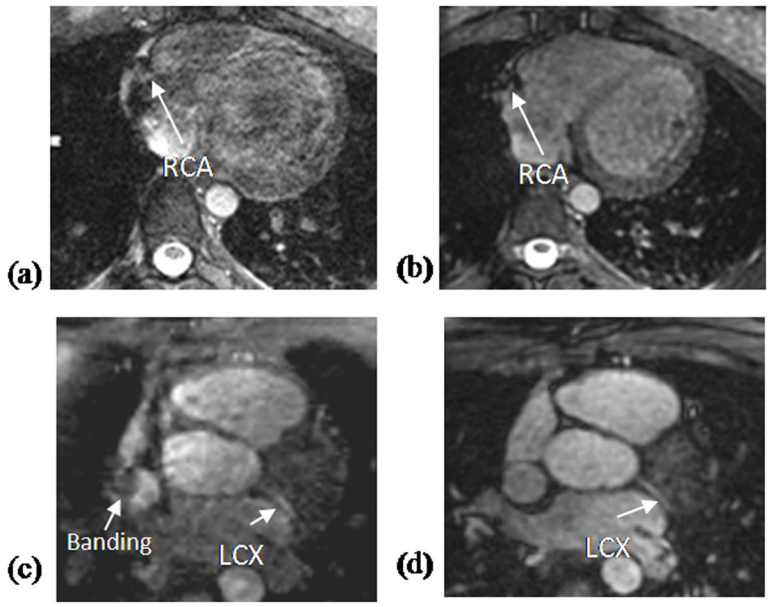

Figure 3.
Comparison between Cartesian (a, c) and VIPR (b, d) trajectory in two healthy volunteers. The Cartesian images (a, c) show severe off-resonance artifacts and poor image quality. In contrast, the VIPR images (b, d) show no obvious artifacts, have homogeneous blood pool signal, good image quality and sharp depiction of the LAD and LCX.

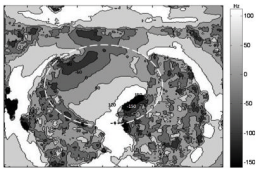

Figure 4.

Off-resonance frequency map with contour lines in one sample slice from a volunteer. A low-pass filter was applied to the frequency map before contouring to reduce the sharp phase change in the region of air. Frequency ranges from -167 Hz to 149 Hz in the heart region (the dashed circle) of this chosen slice.

Table 1

Lengths of major coronary arteries visualized and image sharpness with the VIPR SSFP and Cartesian SSFP sequence. Data are presented as mean ± standard deviation.

Quantitative analysis	Vessel length (cm)				Sharpness (mm^{-1})
	LAD	LCX	RCA	LM	
VIPR SSFP	10.13 ± 0.79	7.90 ± 0.91	7.50 ± 1.65	1.84 ± 0.23	0.81 ± 0.11
Cartesian SSFP	1.57 ± 2.02	1.54 ± 1.93	0.94 ± 1.17	0.46 ± 0.53	0.61 ± 0.13